RSC Advances

ROYAL SOCIETY OF CHEMISTRY

www.rsc.org/advances

Ultralight and Flexible Supercapacitor Electrodes Made from the $Ni(OH)_2$ Nanosheets doped with Ag Nanoparticles/3D Graphene Composite

Wei Lan[a,b,*],Yaru Sun[a], Youxin Chen[a], Junya Wang[a], Guomei Tang[a], Wei Dou[c], Qing Su[a], Erqing Xie[a]

a, School of Physical Science and Technology, Lanzhou University, Lanzhou, 730000, People's Republic of China

b, State Key Laboratory of Advanced Processing and Recycling of Non-ferrous Metals, Lanzhou University of Technology, 730050 Lanzhou, People's Republic of China

c, College of Chemistry and Chemical Engineering, Lanzhou University, Lanzhou 730000, People's Republic of China

E-mail: (W. Lan) lanw@lzu.edu.cn

ABSTRACT:

Composite of the $Ni(OH)_2$ nanosheets doped with Ag nanoparticles/3D graphene($Ag/Ni(OH)_2$/3DG) was synthesized by a combination of chemical vapor deposition and a hydrothermal process. The $Ag/Ni(OH)_2$/3DG composite is light, flexible and has a high conductivity. They can be utilized directly as the supercapacitor electrodes (including current collectors) without using the binder materials or conductive agents. Doping the $Ni(OH)_2$ nanosheets with Ag nanoparticles can improve the conductivity, which enhances the specific capacitance of the hybrid electrode accordingly. Electrochemical tests show a high specific

capacitance of 2167 F/g scaled to the total mass of the electrodes at 10 A/g current density, a good rate capability and an excellent cycling performance of 98% capacitance retention over 1000 cycles at 25 A/g current.

1. Introduction

Growing demand for the renewable energy and the environmental concerns has been leading to the development of the novel energy storage technologies [1-2]. Supercapacitors, also known as electrochemical capacitors, have been researched extensively owing to their high power density and long cycling. Pseudocapacitors (one type of supercapacitors), which can store the energy via a reversible faradaic redox reaction at the electrode surface, are considered as the promising candidates for the energy storage systems [3]. The research results show that the good performance of the electrochemical capacitors usually originates from the high specific surface area as well as the highly reversible reaction of the electrode material [4]. Currently, the most attractive materials as the pseudocapacitors have been the cheap transition metal oxides or hydroxides and conductive polymers [5-10]. However, they often result in compromises in the rate capability and the reversibility. The reason is the limitation of the redox kinetics by the rate of ion diffusion and electron transfer [11-12]. The large specific surface area and high electrical conductivity can improve the capacitance performance of the electrode materials. Nickel (II) hydroxide, $Ni(OH)_2$, shows strong redox properties [13]. It is commonly used in rechargeable battery electrodes by oxidation to nickel (III) oxide-hydroxide. Blocks of $Ni(OH)_2$ have low specific surface area values and low electrical conductivities because of their semiconductive nature, which limit their application as the electrode materials of the electrochemical capacitors. Therefore, nickel hydroxide with a large specific surface area and a high electrical conductivity is sought. Previous studies demonstrated the synergistic effect produced by integrating multiple components,

which could overcome the limitations of the pseudo-materials (e.g. low conductivity of metal oxides and hydroxides) and improve specific capacitance [14-16].

Nickel hydroxide nanosheets show distinctive physicochemical properties as well as large specific surface area values. They can be obtained by hydrothermal reactions or chemical bath deposition and can be employed as supcapacitor electrode material with the capacitance of 1440 F/g at the current density of 10 A/g [17] and high-rate redox activity up to 500 V/s [13]. However, their low electrical conductivity limits further improvements of the electrochemical properties [18]. Some investigations show that the performance of the lithium-ion battery can be significantly improved by doping with 1-8 wt% Ag [19], where Ag nanoparticles can improve the proton diffusion throughout the electrodes [20]. Therefore, Ag-doped $Ni(OH)_2$ nanomaterials are expected to improve the conductivity of the electrodematerial and show a higher specific capacitance by forming electron transfer channels during the the charge/discharge times.

In this work, a simple two-step approach was applied to grow hybrid $Ni(OH)_2$ nanosheets doped with Ag nanoparticles/3D graphene composite. The first step is to grow 3D graphene on the nickel foam using a CVD technique, which is considered as the most effective way to fabricate graphene films with a large surface area and a high quality. The second stage is the synthesis of the $Ni(OH)_2$ nanosheets doped with Ag on the as-prepared 3D graphene. Furthermore, the electrochemical properties of the products and the mechanism of formation were analyzed.

2. Experimental

2.1. Materials

All the reagents used in this work were analytical grade and were used without further purification and treatment. Nickel nitrate ($Ni(NO_3)_2 \cdot 6H_2O$), hexamine,

hydrogen chloride (HCl) were purchased from Sigma Aldrich Co. LLC. Nickel (Ni) foams were purchased from Shanghai Zhongwei New Material Co.Ltd., China. Ag nanoparticles were obtained from Suzhou ColdStones Technology Co. Ltd. Deionized water was used in the experiments.

2.2. Equipment

The morphologies of the samples were characterized by field emission scanning electron microscopy (FE-SEM, Hitachi S-4800) with an accelerating voltage of 5 kV. The microstructures were characterized using transmission electron microscopy (TEM, FEI Tecnai F30, operated at 300 kV) equipped with an X-ray energy dispersive spectrometer (EDS). Samples were prepared by immerging the Ag/$Ni(OH)_2$/3DG materials in ethanol, followed by an ultrasonic treatment. The suspension was then dropped on the carbon-coated copper grids and dried in air at room temperature for observation. The crystal structures of the products were examined by X-ray diffraction (XRD, Philips, X'pert pro, Cu Kα, 0.154056 nm) and Raman spectroscopy (JY-HR800 micro-Raman, using a 532 nm wavelength YAG laser with a laser spot diameter of ~600 nm). The mass of Ag/$Ni(OH)_2$ active materials was measured by a microbalance (Mettler, XS105DU) with an accuracy of 0.01 mg.

Electrochemical measurements (CHI 660E Electrochemical Workstation) were conducted in a three-electrode electrochemical cell at room temperature in a 1 M NaOH aqueous electrolyte. The Ag/$Ni(OH)_2$/3DG hybrid nanostructures were used directly as the working electrodes. A Pt plate and an Hg/HgO electrode were used as the counter electrode and the reference electrode, respectively. The nominal area of the Ag/$Ni(OH)_2$/3DG immersed into the electrolyte was controlled to be at around 1 cm×1 cm. All the potentials were referred to the reference electrode.

2.3. Synthesis

The composite of the $Ni(OH)_2$ nanosheets doped with Ag nanoparticles/3D graphene was fabricated by a two-step approach:

In the first stage, 3D graphene was synthesized by a CVD method. A part of the nickel foam was placed at the center of the quartz tube, which was mounted in the high-temperature furnace. Prior to heating, 100 sccm Ar and 50 sccm H_2 were introduced for 15 min to evacuate the air from the system. Then, the nickel foam was heated to 1000°C in 60 min under Ar (100 sccm) and H_2 (50 sccm). The temperature was then maintained at 1000 °C for 30 min. The H_2 flow was then reduced to 20 sccm and the ethanol was introduced into the reaction tube as the carbon source simultaneously. After 20 min, the ethanol flow was stopped and the furnace was cooled down under Ar and H_2. The Ni foams were then eliminated by 3 mol/L HCl aqueous solution at 80 °C to gain a free-supporting 3D graphene.

In the second stage, Ag-doped $Ni(OH)_2$/graphene nanosheets were prepared by a hydrothermal method. 0.201 g of $Ni(NO_3)_2 \cdot 6H_2O$, 0.504 g of hexamine and 2 mg of Ag nanoparticles (1 mg/mL) were dissolved in 35 mL deionized water. Then the mixture was stirred on a magnetic stirrerfor 2 h at room temperature. The mixture was then transferred into a Teflon-lined stainless steel autoclave and the 3D graphene foam was placed into the solution. The autoclave was sealed and kept at 80 °C for 8 h. Then, the system was cooled down to the room temperature under natural conditions. The sample was washed with deionized water 3 times and was dried at 65 °C for 3 h.

3. Results and Discussion

The as-prepared 3D graphene foams are thin, flexible and hold ultralight weight

architectures. Fig. 1 shows the fabrication process of the Ag/$Ni(OH)_2$/3DG composite. As can be seen from the photographs, the as-prepared 3D free-standing graphene is quite light (~0.6 mg/cm^2), which can be caught by a glass rod due to the electrostatic force and can be bent by the tweezers. For the synthesis process of the active material on the 3DG, the main chemical reactions involved in the formation of $Ni(OH)_2$ nanosheets are as follows:

$$Ni^{2+} + xNR_3 + (6\text{-}x)H_2O \leftrightarrow [Ni(NR_3)_x \cdot (H_2O)_{6-x}]^{2+} \quad (1)$$

$$[Ni(NR_3)_x \cdot (H_2O)_{6-x}]^{2+} \xleftrightarrow{\Delta} [Ni(OH)(H_2O)_{5-x}(NR_3)_{x-1}]^{+} + HNR_3^{+} \quad (2)$$

$$Ni(OH)(H_2O)_{5-x}(NR_3)_{x-1} \leftrightarrow Ni(OH)_2(H_2O)_{4-x}(NR_3)_{x-2} + HNR_3^{+} \quad (3)$$

$$Ni(OH)_2(H_2O)_{4-x}(NR_3)_{x-2} \leftrightarrow Ni(OH)\downarrow + (4\text{-}x)H_2O + (x\text{-}2)NR_3 \quad (4)$$

The Ag nanoparticles were encapsulated in the $Ni(OH)_2$ nanosheets during the synthesis process.

XRD characterization was used to study the hybrids (Fig. 2a). The peaks corresponding to the $Ni(OH)_2$ (JCPDS no.14-0117), Ag (JCPDS no.04-0783) nanoparticles and the graphene were detected [7]. The results suggest the coexistence of the Ag, $Ni(OH)_2$ and 3DG phases. Fig. 2b shows the Raman spectra of the 3D graphene and Ag/$Ni(OH)_2$/3DG composite. In both of the samples, the G peak at ~1580 cm^{-1} corresponds to the vibration of carbon atoms in the hexagonal graphene lattice and 2D peak at ~2716 cm^{-1} correspond to the second order of zone-boundary phonons. No D peak related to the defects was detected. This confirms the good quality of graphene foam and further implies a good conductivity that is very important for supercapacitors electrodes [21-22]. When compared with the spectrum of the 3D graphene, Ag/$Ni(OH)_2$/3DG spectrum also displays a peak at ~510 cm^{-1}, which can be attributed to the $Ni(OH)_2$ nanosheets. This indicates that the hybrids are synthesized successfully.

$Ni(OH)_2$ nanosheets doped with Ag nanoparticles grown on the 3D graphene were prepared by a simple hydrothermal reaction. The SEM images are shown in Fig. 3, which show that the $Ni(OH)_2$ nanosheets are uniformly coated onto the graphene foam forming a 3D network structure. Fig. 3b and 3c are magnified images of this region, which shows that the $Ni(OH)_2$ nanosheets are in a layered structure following the same pattern. These nanosheets are interconnected sheets that are deposited vertically on the whole graphene foam surfaces and the sheet has a direct contact with the 3D graphene. Thus, the hybrid can be used directly as the electrodes (including current collectors), without involving the other less active materials such as binders and conductive additives. Besides, this structure facilitates the ion diffusion, enlarges the contact area with the electrolyte and then increases the utilization of pseudocapacitance materials. The magnified image (Fig. 3d) of the nanosheets shows that the size and thickness of the nanosheets are highly uniform. $Ni(OH)_2$ nanosheets doped with Ag nanoparticles are adhered firmly to the 3D graphene.

TEM images of the $Ag/Ni(OH)_2/3DG$ samples are presented in Fig. 4a and 4b. It is shown that $Ni(OH)_2$ nanosheets are thin transparent platelets, which are adhered firmly to the 3D graphene. The inset in Fig. 4b shows that the Ag nanoparticles are kept stable on the nanosheets. The SEM images do not show any nanoparticles. Therefore, we conclude that Ag nanoparticles are encapsulated in the $Ni(OH)_2$ nanosheets. High resolution TEM image in Fig. 4c reveals three interplanar spacings of 0.234, 0.209 and 0.232 nm, corresponding to (101) lattice plane of $Ni(OH)_2$, (200) and (111) ones of Ag, respectively. Energy dispersive X-ray spectroscopy (EDS) analysis is shown in Fig. 4d. It also reveals that Ag nanoparticles are encapsulated in the $Ni(OH)_2/3DG$ composite.

To investigate the supercapacitor applications of these hybrid architectures, the electrochemical tests were performed. Fig. 5a shows the comparison of the cyclic voltammetry (CV) curves of the $Ag/Ni(OH)_2/3DG$ composite (black) and the $Ni(OH)_2/3DG$ composite (red) under the same conditions. The potential window is

restricted in a range of 0-0.7 V versus a Hg/HgO reference electrode. It is apparent that the Ag/$Ni(OH)_2$/3DG hybrid electrode (black) shows a better performance. Furthermore, Fig. 5b displays the comparison between the galvanostatic charge/discharge curves for the Ag/$Ni(OH)_2$/3DG hybrid electrode (black) and the $Ni(OH)_2$/3DG hybrid electrode (red) at the same current density of 10 A/g. Evidently, the charge/discharge times of the $Ni(OH)_2$/3DG composite are shorter than those of the Ag/$Ni(OH)_2$/3DG composite.

Fig. 6a shows the cyclic voltammetry (CV) curves of the Ag/$Ni(OH)_2$/3DG composite electrodes at different scan rates of 5, 10, 15, 20, 30, 40 and 50 mV/s. The anodic peak (positive current density) indicates an oxidation process related to the oxidation of α-$Ni(OH)_2$ to γ-NiOOH, whereas the cathodic peak (negative current density) corresponds to a reduction process following the Faradaic reactions of $Ni(OH)_2$, see Equation (5).

$$\alpha\text{-}Ni(OH)_2 + OH^- \leftrightarrow \gamma\text{-}NiOOH + H_2O + e^- \quad (5)$$

The intensity of the current peak increases with negligible change in the shape of the CV curves as the scan rates increase from 5 to 50 mV/s. This reveals a good electrochemical reversibility and the high power capabilities. The specific capacitance value, *Cs*, can be estimated according to Equation (6).

$$Cs = It/(m\Delta V) \quad (6)$$

Where I is the current density, t is the charge/discharge time, ΔV is the potential window and m is the mass of the active material. Fig. 6b displays the galvanostatic charge/discharge curves of the hybrid structures at the different current densities of 10, 20, 25, 30, 40, 60 and 80 A/g. The calculated capacitance values are shown in Fig. 6c. The *Cs* of the Ag/$Ni(OH)_2$/3DG composite electrodeis obtained to be ~2167 F/g at a charge/discharge current density of 10 A/g. For the undoped $Ni(OH)_2$ nanosheets, the calculated *Cs* is 1766 F/g at the same current density of 10 A/g. Therefore, by

doping the silver nanoparticles, the specific capacitance of the $Ni(OH)_2$supercapacitor electrodes is improved by ~23%. The *Cs* of the Ag/$Ni(OH)_2$/3DG can reach the value of 1333 F/g at the charge/discharge current density of 80 A/g. The specific capacitance decreases gradually as the current density increases. When thecharge/discharge current density increases from 10 to 80 A/g, ~62% of the capacitance is still remained. The capacitance value is also higher than the reported results. Ghosh *et al.*, [18] synthesized hierarchical stacked nanoplate of Ag-deposited $Ni(OH)_2$/graphene composite with maximum specific capacitance of 496 F/g at 1 A/g current density accompanying 93 % specific capacitance retention at the end of 500 consecutive charge discharge cycles. Wu *et al.,* [23] grew $Ni(OH)_2$ on the graphene as the electrode. They obtained the highest specific capacitance of 1503 F/g at the scan rate of 2 mV/s by integrating the area under the CV curves. Bag *et al.,* [24] obtained a specific capacitance of 1339.13 F/g for the layered hybrid rGO/α-$Ni(OH)_2$ electrodes at a current density of 10 A/g. Ma *et al.,* [25] prepared a 3D flower-like β-$Ni(OH)_2$/GO/CNTs composite and found that the specific capacitance based on the mass of $Ni(OH)_2$ was ~1060 F/g at 10 A/g. Our specific capacitance results show an increase of ~ 45%, when compared with the highest reported capacitance value of ~1500 F/g. The cycling stability of the hybrid electrode was also examined over 1000 charge/discharge cycles at the current density of 25 A/g, which shows that over 98 % of the capacitance is maintained (Fig. 6d). Besides, after 1000 cycles, no change in the curves (inset) was detected, which reveals a good cycling performance.

Electrochemical impedance can be used to describe the resistance characteristic. Electrochemical impedance spectroscopy (EIS) data of the $Ni(OH)_2$/3DG and Ag/$Ni(OH)_2$/3DG composite are shown in Fig. 7. The Nyquist plots of the two materials are similar to each other with a semicircle at the higher frequency region and a spike at the lower frequency. The semicircle at the high-frequency range is due to the charge transfer reaction at the interface of the electroyte/oxide electrode. It corresponds to the charge transfer resistance (R_{ct}) and can be calculated by

extrapolation of the semicircle on the real impedance axis [26]. The EIS spectra shows that the diameter of the semicircles associated with the Ag/$Ni(OH)_2$/3DG composite decreases. This indicates that the R_{ct} of the Ag/$Ni(OH)_2$/3DG composite (1.8 Ω) is lower than that of the $Ni(OH)_2$/3DG (3.0 Ω) composite and the electrochemical reaction on the electrode/electrolyte interface is easier. This result indicates that the presence of the Ag nanoparticles indeed decreases the electrical resistivity of the electrode. In addition, the inclined line in the low frequency range is attributed to the Warburg impedance, resulting from the frequency dependence of the ion diffusion and the transport in the electrolyte [27]. It is obvious that the linear region of the plots forms an angle relative to the real axis. The angle of the line associated with the Ag/$Ni(OH)_2$/3DG composite is lower than that of the $Ni(OH)_2$/3DG composite. This result shows that the Ag/$Ni(OH)_2$/3DG composite can improve the electrical performance by increasing the conductivity.

4. Conclusions

We applied a simple and effective approach to synthesize 3D graphene foam holding a high conductivity and a light weight. We then integrated the structures with the $Ni(OH)_2$ nanosheets to be served as the supercapacitor electrodes for energy storage applications. To improve the poor conductivity of the $Ni(OH)_2$, the Ag nanoparticles were introduced. In these unique structures, the presence of the 3D graphene and the Ag nanoparticles allows the efficient use of the $Ni(OH)_2$ pseudocapacitors for charge storage. This facilitates the transport of the electrolyte ions and the electrons, which provides a high specific capacitance and a good cycling performance.

Acknowledgements

This work was support by Natural Science Foundation of Gansu Province (No.1208RJZA199), the fund of the State Key Laboratory of Advanced Processing and Recycling of Non-ferrous Metals, Lanzhou University of Technology (SKLAB02014003) and the Project-sponsored by SRF for ROCS, SEM.

References

[1] P. Simon, Y. Gogotsi, Materials for electrochemical capacitors, Nature Mater. 2008, **7**, 845-854.

[2] P Si, S. J. Ding, X. W. Lou, D. H. Kim, An electrochemically formed three-dimensional structure of polypyrrole/graphene nanoplatelets for high-performance supercapacitors, RSC Adv., 2011, **1**, 1271-1278.

[3] B. E. Conway, V. Birss, J. Wojtowicz, The role and utilization of pseudocapacitance for energy storage by supercapacitors, J. Power Sources, 1997, **66**,1-14.

[4] C. -C. Hu, K. -H. Chang, M. C. Lin, Y. T. Wu, Design and tailoring of the nanotubular arrayed architecture of hydrous RuO_2 for next generation supercapacitors, Nano Lett., 2006, **12**, 2690-2695.

[5] G. Yang, C. Xu, H. Li, Electrodeposited nickel hydroxide on nickel foam with ultrahigh capacitance, Chem. Commun. 2008, **48**, 6537-6539

[6] K. -W. Nam, K. -H. Kim, E. -S. Lee, W. -S. Yoon, X. -Q. Yang, K. -B. Kim, Pseudocapacitive properties of electrochemically prepared nickel oxides on 3-dimensional carbon nanotube film substrates, J. Power Sources, 2008, **182**, 642-652.

[7] W. Deng, W. Lan, Y. R. Sun, Q. Su, E. Q. Xie, Porous CoO nanostructures grown

on three-dimension graphene foams for supercapacitors electrodes, Appl. Surf. Sci., 2014, **305**, 433-438. W. Deng, Y. R. Sun, Q. Su, E. Q. Xie, W. Lan, Porous CoO nanobundles composited with 3D graphene foams for supercapacitors electrodes, Mater. Lett., 2014, **137**,124-127.

[8] M. E. Roberts, D. R. Wheeler, B. B. McKenzie, B. C. Bunker, High specific capacitance conducting polymer supercapacitor electrodes based on poly(tris(thiophenylphenyl)amine), J. Mater. Chem., 2009, **19**,6977-6979.

[9] K. Zhang, L. L. Zhang, X. S. Zhao, J. Wu, Graphene/Polyaniline Nanofiber Composites as Supercapacitor Electrodes, Chem. Mater., 2010 **22** 1392-1401.

[10] Z. Khan, S. Bhattu, S. Haramb, D. Khushalani, SWCNT/$BiVO_4$ composites as anode materials for supercapacitor application, RSC Adv., 2014, **4**, 17378-17381.

[11] R. Kötz, M. Carlen, Principles and applications of electrochemical capacitors, Electrochim. Acta., 2000, **45**, 2483-2498.

[12] J. Liu, C. Cheng, W. Zhou, H. Li, H. J. Fan, Ultrathin nickel hydroxidenitrate nanoflakes branched on nanowire arrays for high-rate pseudocapacitive energy storage, Chem. Commun., 2011, **47**, 3436-3438.

[13] N. Kurra, N. A. Alhebshi, H. N. Alshareef, Microfabricated pseudocapacitors using $Ni(OH)_2$ electrodes exhibit remarkable volumetric capacitance and energy density, Adv. Energy Mater., 2015, **5**, 1401303.

[14] J. Yan, Z. J. Fan,W. Sun, G. Q. Ning, T. Wei, Q. Zhang, R. F. Zhang, L. J. Zhi, F. Wei, Adcanced asymmetric supercapacitors based on $Ni(OH)_2$/graphene and porous graphene electrodes with high energy density, Adv. Funct. Mater., 2012, **22**, 2632-2641.

[15] Q. Li, Z. L. Wang, G. R. Li, R. Guo, L. X. Ding, Y. X. Tong, Nanotube arrays with high supercapacitive performance for electrochemical energy storage, Nano

Lett., 2012, **12**, 3803-3807.

[16] J. Y. Ji, L. L. Zhang, H. X. Ji, Y. Li, X. Zhao, X. B. Fan, F. B. Zhang, R. S. Ruoff, Nanoporous $Ni(OH)_2$ thin film on 3D ultrathin-graphite foam for asymmetric supercapacitor, ACS Nano., 2013, **7**, 6237-6243.

[17] T. Xiao, B. Heng, X. Chen, $Ni(OH)_2$ nanosheets grown on graphene-coated nickel foam for high-performance pseudocapacitors, J Alloys Compd., 2013, **549**, 147-151.

[18] D. Ghosh, S. Giri, A. Mandal, C. K. Das, Graphene decorated with $Ni(OH)_2$ and Ag deposited $Ni(OH)_2$ stacked nanoplate for supercapacitor application, Chem. Phys. Lett., 2013, **573**, 41-47.

[19] X. M. Wu, Z. Q. He, S. Chen, M. Y. Ma, Z. B. Xiao, J. B. Liu, Silver-doped lithium manganese oxide thin films prepared by solution deposition, Mater. Lett., 2006, **60**, 2497-2500.

[20] S. Wang, J. Xie, T. Zhang, V. K. Varadan, Silver decorated γ-manganese dioxide nanorods for alkaline battery cathode, J. Power Sources, 2009, **186**, 532-538.

[21] S. J. Chae, F. Guenes, K. K. Kim, E. S. Kim, G. H. Han, S. M. Kim, H. -J. Shin, S. -M. Yoon, J. -Y. Choi, M. H. Park, C. W. Yang, D. Pribat, Y. H. Lee, Synthesis of large area graphene layers on poly-nickel substrate by chemical vapor deposition: wrinkel formation, Adv. Mater., 2009, **21**, 2328-2333.

[22] A. C. Ferrari, J. C. Meyer, V. Scardaci, C. C. asiraghi, M. Lazzeri, F. Mauri, S. Piscanec, D. Jiang, K. S. Novoselov, S. Roth, A. K. Geim, Raman spectrum of graphene and graphene layers, Phy. Rev. Lett., 2006, **97**, 187401.

[23] Z. Wu, X. L. Huang, Z. L. Wang, J. J. Xu, H. G. Wang, X. B. Zhang, Electrostatic induced stretch growth of homogeneous β-$Ni(OH)_2$ on graphene with enhanced high-rate cycling for supercapacitors, Sci. Rep. 2013, **4**, 3669.

[24] S. Bag, C. R. Raj, Layered inorganic-organic hybrid material based on reduced graphene oxide and α-$Ni(OH)_2$ for high performance supercapacitor electrodes, J. Mater. Chem. A, 2014, **2**, 17848-17856.

[25] X. W. Ma, J. W. Liu, C. Y. Liang, X. W. Gong, R. C. Che, A facile phase transformation method for the preparation of 3D flower-like β-$Ni(OH)_2$/GO/CNTs composite with excellent supercapacitor performance, J. Mater. Chem., 2014, **2**, 12692-12696

[26] M. Ghaemi, F. Makhlooghi, H. Adelkhani, M. Aghazadeh, H. M. Shiri, The influence of electroless silver deposition on electrochemical properties of the steel cathode current collector of alkaline batteries, Int. J. Electrochem. Sci., 2010, **5**, 131-146.

[27] X. Du, P. Guo, H. Song, X. Chen, Graphene nanosheets as electrode material for electric double-layer capacitors, Electrochim. Acta., 2010, **55**, 4812-4819.

Figure captions

Fig 1. Schematics of the fabrication process of the Ag/$Ni(OH)_2$/3DG composite.

Fig 2.(a) XRD pattern of 3D graphene after hydrothermal process; (b) The typical Raman spectra of the Ag/$Ni(OH)_2$/3DG composite (red) and the graphene (black).

Fig 3.SEM images of Ag/$Ni(OH)_2$/3DG hybrid electrodes at different magnifications.

Fig 4. (a) and (b) TEM images of the Ag/$Ni(OH)_2$/3DG hybrid electrodes. The inset in (b) is the high magnification of the nanosheets; (c) The HRTEM images of the $Ni(OH)_2$ and Ag crystal lattice; (d) The EDS spectrum of the Ag/$Ni(OH)_2$/3DG composite.

Fig 5. (a) CV curves of the Ag/$Ni(OH)_2$/3DG composite (Black) and $Ni(OH)_2$/3DG composite (Red) at the same scan rate of 20 mV/s; (b) The galvanostatic charge/discharge curves of the Ag/$Ni(OH)_2$/3DG composite (Black) and the $Ni(OH)_2$/3DG composite(Red) at the same current density of 10 A/g.

Fig 6.(a) CV curves of the Ag/$Ni(OH)_2$/3DG composite as the electrode at various scan rates; (b) Galvanostatic charge/discharge curves at various current densities; (c) The calculated capacitance as a function of current density; (d) Cycling performance of the Ag/$Ni(OH)_2$/3DG hybrid structures over 1000 cycles at the current density of

25 A/g. The inset is showing the single charge/discharge curves before and after 1000 cycles.

Fig 7. (a) The EIS spectra of the $Ni(OH)_2$/3DG and Ag/$Ni(OH)_2$/3DG composite with a frequency range from 0.5 to 10^5 Hz in a 1 M NaOH aqueous electrolyte; the inset is the equivalent circuit. (b) The diagram of the three-electrode cell.

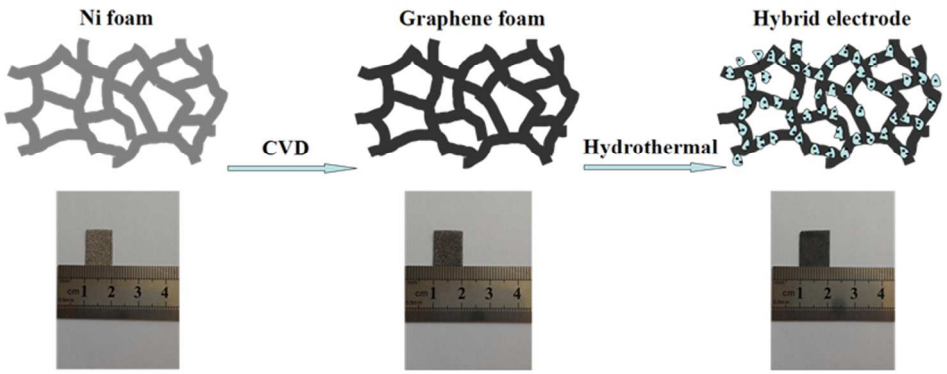

Fig 1. Schematics of the fabrication process of the Ag/Ni(OH)2/3DG composite.
72x31mm (300 x 300 DPI)

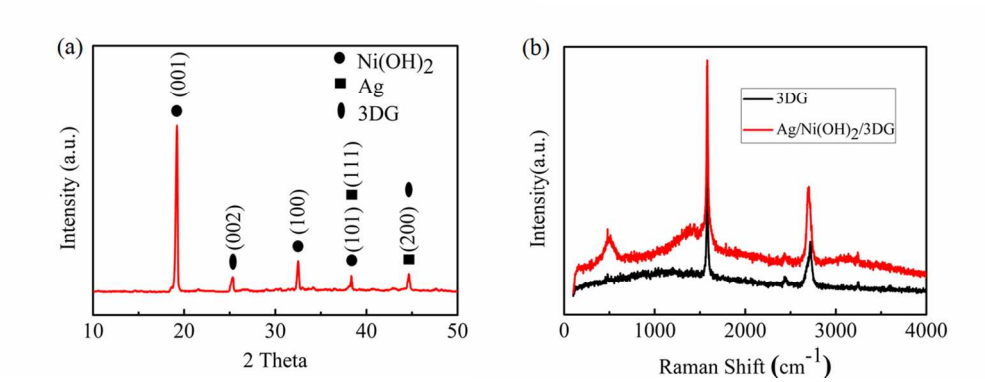

Fig 2.(a) XRD pattern of 3D graphene after hydrothermal process; (b) The typical Raman spectra of the Ag/Ni(OH)2/3DG composite (red) and the graphene (black).
123x46mm (300 x 300 DPI)

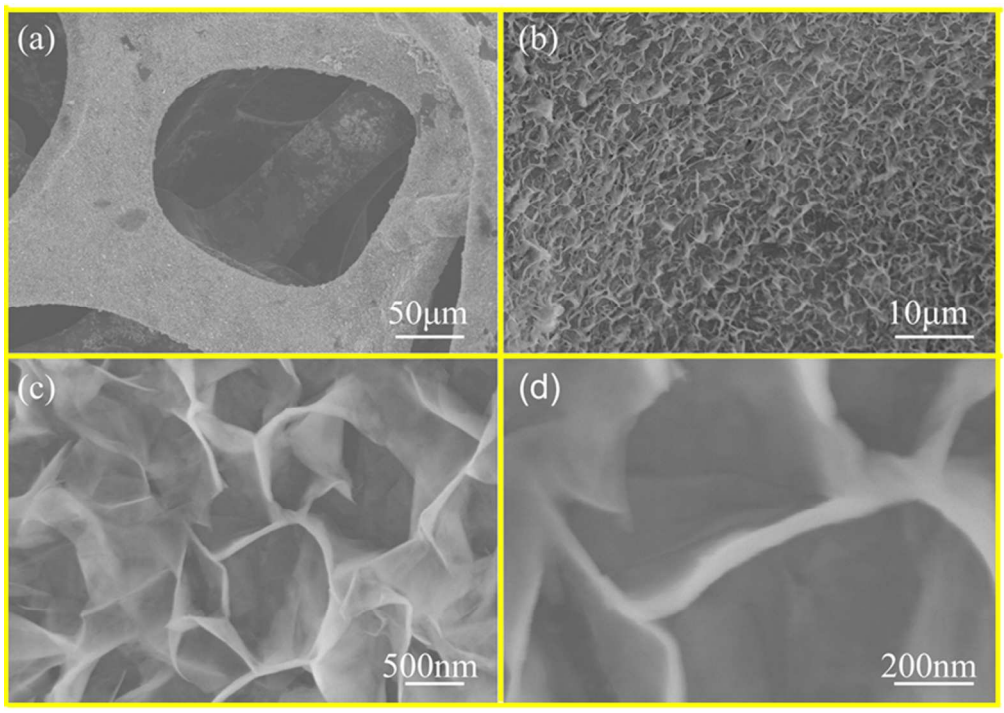

Fig 3.SEM images of Ag/Ni(OH)2/3DG hybrid electrodes at different magnifications.
70x49mm (300 x 300 DPI)

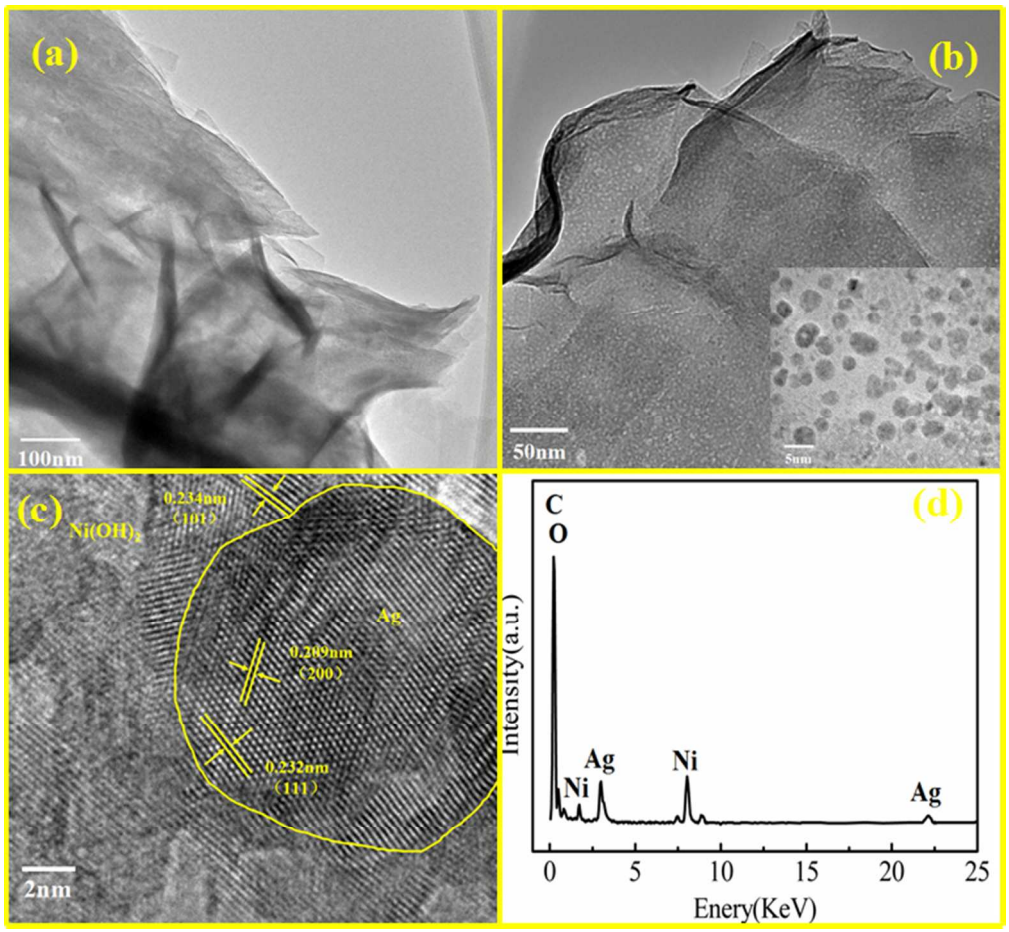

Fig 4. (a) and (b) TEM images of the Ag/Ni(OH)2/3DG hybrid electrodes. The inset in (b) is the high magnification of the nanosheets; (c) The HRTEM images of the Ni(OH)2 and Ag crystal lattice; (d) The EDS spectrum of the Ag/Ni(OH)2/3DG composite.
64x59mm (300 x 300 DPI)

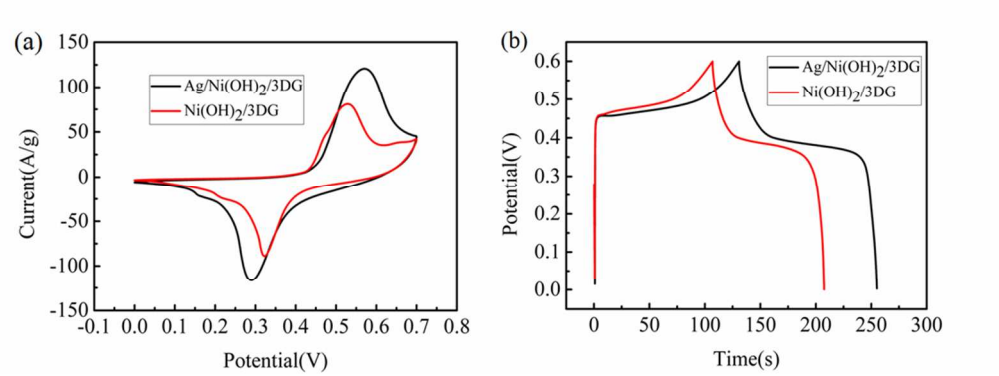

Fig 5. (a) CV curves of the Ag/Ni(OH)2/3DG composite (Black) and Ni(OH)2/3DG composite (Red) at the same scan rate of 20 mV/s; (b) The galvanostatic charge/discharge curves of the Ag/Ni(OH)2/3DG composite (Black) and the Ni(OH)2/3DG composite(Red) at the same current density of 10 A/g.
96x35mm (300 x 300 DPI)

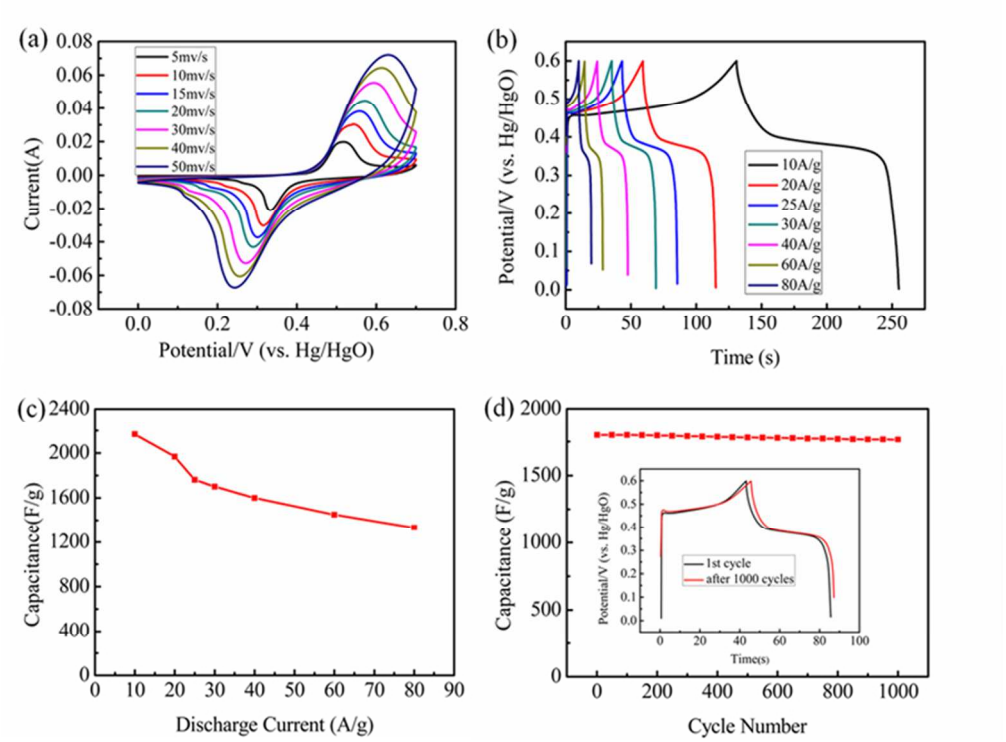

Fig 6.(a) CV curves of the Ag/Ni(OH)2/3DG composite as the electrode at various scan rates; (b) Galvanostatic charge/discharge curves at various current densities; (c) The calculated capacitance as a function of current density; (d) Cycling performance of the Ag/Ni(OH)2/3DG hybrid structures over 1000 cycles at the current density of 25 A/g. The inset is showing the single charge/discharge curves before and after 1000 cycles.
76x56mm (300 x 300 DPI)

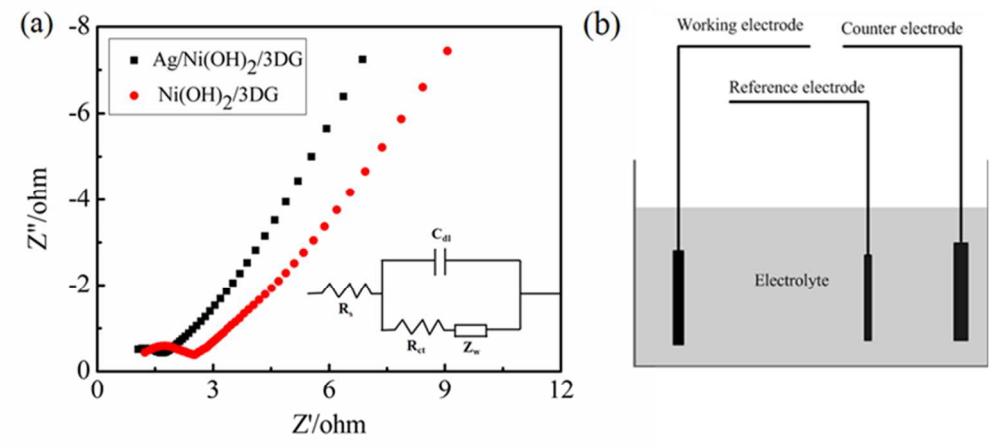

Fig 7. (a) The EIS spectra of the Ni(OH)2/3DG and Ag/Ni(OH)2/3DG composite with a frequency range from 0.5 to 105 Hz in a 1 M NaOH aqueous electrolyte; the inset is the equivalent circuit. (b) The diagram of the three-electrode cell.
66x32mm (300 x 300 DPI)